1474 *Biochemistry* **2011,** *50,* 1474–1482
DOI: 10.1021/bi1013535

BIOCHEMISTRY
including biophysical chemistry & molecular biology
Article

Substrate Specificity and Catalysis by the Editing Active Site of Alanyl-tRNA Synthetase from *Escherichia coli* †

Zvi Pasman,‡ Susan Robey-Bond, Adam C. Mirando, Gregory J. Smith, Astrid Lague, and Christopher S. Francklyn*

Department of Biochemistry, College of Medicine, Health Sciences Complex, 89 Beaumont Avenue, University of Vermont, Burlington, Vermont 05405, United States. ‡Current address: Department of Chemistry, Illinois College, 1101 W. College Ave., Jacksonville, IL 62650

Received August 20, 2010; Revised Manuscript Received January 10, 2011

ABSTRACT: Aminoacyl-tRNA synthetases (ARSs) enhance the fidelity of protein synthesis through multiple mechanisms, including hydrolysis of the adenylate and cleavage of misacylated tRNA. Alanyl-tRNA synthetase (AlaRS) limits misacylation with glycine and serine by use of a dedicated editing domain, and a mutation in this activity has been genetically linked to a mouse model of a progressive neurodegenerative disease. Using the free-standing *Pyrococcus horikoshii* AlaX editing domain complexed with serine as a model and both Ser-tRNA^{Ala} and Ala-tRNA^{Ala} as substrates, the deacylation activities of the wild type and five different *Escherichia coli* AlaRS editing site substitution mutants were characterized. The wild-type AlaRS editing domain deacylated Ser-tRNA^{Ala} with a k_{cat}/K_M of 6.6×10^5 M^{-1} s^{-1}, equivalent to a rate enhancement of 6000 over the rate of enzyme-independent deacylation but only 12.2-fold greater than the rate with Ala-tRNA^{Ala}. While the E664A and T567G substitutions only minimally decreased k_{cat}/K_M, Q584H, I667E, and C666A AlaRS were more compromised in activity, with decreases in k_{cat}/K_M in the range of 6-, 6.6-, and 15-fold. C666A AlaRS was 1.7-fold more active on Ala-tRNA^{Ala} relative to Ser-tRNA^{Ala}, providing the only example of a true reversal of substrate specificity and highlighting a potential role of the coordinated zinc in editing substrate specificity. Along with the potentially serious physiological consequences of serine misincorporation, the relatively modest specificity of the AlaRS editing domain may provide a rationale for the widespread phylogenetic distribution of AlaX free-standing editing domains, thereby contributing a further mechanism to lower concentrations of misacylated tRNA^{Ala}.

Aminoacyl-tRNA synthetases (ARS)[1] join amino acids to their cognate tRNAs in a two-step ATP-dependent reaction:

$$AA + ATP \xrightarrow{ARS/Mg^{2+}} AA{\sim}AMP + PP_i \quad (1)$$

$$AA{\sim}AMP + tRNA \xrightarrow{ARS} AA\text{-}tRNA + AMP \quad (2)$$

The amino acid is first condensed to form an enzyme-bound adenylate, accompanied by release of pyrophosphate. In the second step, the amino acid undergoes transfer to the tRNA. The aminoacylation reaction is catalyzed by two evolutionarily unrelated classes of ARS enzymes, and these are distinguished by a unique catalytic fold, characteristic signature sequences, and regiochemistry of aminoacyl transfer (*1*). In a typical cell, there are generally at least 20 such enzymes, one for each of the standard amino acids in protein synthesis. The existence of two distinct classes of enzymes that catalyze the same reaction raises the issue of whether common or distinct mechanisms are in place to maximize both catalytic efficiency and substrate specificity.

The translation process is characterized by a defined error rate of 10^3–10^4 per site per generation, with the decoding process representing the step with the highest frequency of errors (*2*). Despite the presence of highly evolved proofreading activities, errors with significant physiological consequences can still occur (*3*) (*4*). The aminoacylation reaction also introduces errors into translation, albeit at a lower error frequency (*5*). Mistranslation can arise as a consequence of mistakes during the selection of either tRNA or amino acid (*6*), but proofreading of tRNA appears not to be necessary for accurate aminoacylation (*7*). The discrimination by ARSs between related amino acids, by contrast, is much more difficult. For pairs of amino acids like valine/isoleucine and glycine/alanine, which differ by only a single methyl group, the amount of binding free energy available for discrimination is in the range of 1 kcal (*8*), equivalent to an error rate of no better than 1 in a 100. Under physiological conditions, the observed error of misacylation is closer to 1 in > 50000, or ~0.0001% (*9*).

The enhanced fidelity of ARSs relative to their theoretically predicted accuracy is rationalized by specialized editing domains that exist in both class I (e.g., IleRS, ValRS, and LeuRS) and class II (e.g., ThrRS, ProRS, PheRS, and AlaRS) ARS enzymes (*10*, *11*). By virtue of its two-step nature, the aminoacylation reaction affords two specific branch points where errors can be corrected (*12*). Preferential hydrolysis of misactivated near-cognate

†This work was supported by NIGMS Grant GM-54899.
*Address correspondence to this author. Tel: 802-656-8450. Fax: 802-656-8229. E-mail: Christopher.Francklyn@uvm.edu.
[1]Abbreviations: AlaRS, alanyl-tRNA synthetase; AlaX, free-standing editing domain derived from AlaRS; ARS, aminoacyl-tRNA synthetase; IleRS, isoleucyl-tRNA synthetase; PheRS, phenylalanyl-tRNA synthetase; ProRS, prolyl-tRNA synthetase; RNAP, RNA polymerase; ThrRS, threonyl-tRNA synthetase; TLC, thin-layer chromatography.

 Published on Web 01/17/2011

amino acids can be removed prior to aminoacyl transfer by a process referred to as "pretransfer editing" (*13*, *14*). Alternatively, near-cognate amino acids can be removed from the cognate tRNA 3′ end after aminoacyl transfer by a deacylation activity that resides in the specialized editing domain distinct from the site of aminoacylation chemistry (*15*, *16*). This latter mechanism is referred to as "posttransfer editing." The existence in numerous taxa of proteins that recapitulate the isolated editing domains of class II aminoacyl-tRNA synthetases suggests that posttransfer editing can occur subsequent to product release of the misacylated tRNA from the cognate ARS (*17*−*19*). In support of this hypothesis, recent work suggests that "resampling" (i.e., dissociation of misacylated tRNA, followed by rebinding to the original ARS) can contribute to overall fidelity (*20*).

As a consequence of the requirement to reject amino acids that are both smaller (i.e., glycine) and larger (i.e, serine) than the cognate, alanyl-tRNA synthetase (AlaRS) is among the ARSs that exhibit amino acid proofreading. Notably, a "double sieve" (*21*) that functions purely on the basis of the volume of the side chain would not be expected to provide the requisite specificity. AlaRS readily activates both glycine and serine, although substantially higher concentrations of the noncognate amino acids are required to detect adenylation activity (*22*). This property provides a presumptive requirement for editing function to eliminate glycyl- and seryl-tRNA^{Ala} from entering protein synthesis.

AlaRS from *Escherichia coli* is a tetramer of four identical subunits, each of which is 875 residues in length (*23*, *24*). AlaRS also possesses a modular structure of linear domains (*25*−*27*) and retains the defining motifs of the class II ARSs (*28*). The tRNA recognition properties of AlaRS have been well studied (*29*, *30*). The anticodon of tRNA^{Ala} is not recognized (*31*), and a strictly conserved G3·U70 base pair in the acceptor stem represents a dominant recognition element for both aminoacylation (*32*, *33*) and editing (*34*). The determination of the structure of the ThrRS−tRNA^{Thr} complex revealed significant sequence similarity between the editing domain of ThrRS and the C-terminal region of AlaRS, implicating the latter as a potential editing domain (*35*). Subsequent biochemical analysis confirmed that the editing activity of AlaRS is localized to this domain, particularly to residues 553−705 (*34*, *36*). In addition, free-standing versions of the AlaRS editing domain (referred to as AlaX proteins) have been identified, several of which exhibit the ability to deacylate mischarged tRNA^{Ala} in vitro (*18*, *37*) and minimize the toxicity associated with mistranslation in vivo (*38*). It has also been reported that a mutation in the AlaRS editing domain (A734E) is genetically linked to degeneration of the Purkinje cell region of the brain in a mouse model of neurodegenerative disease, the so-called "sticky mouse" (*39*). That study concluded that a modest (~2-fold) defect in editing by AlaRS is sufficient to bring about the observed neurodegenerative phenotype.

Here, we examined the amino acid selection properties of alanyl-tRNA synthetase, focusing on the properties of the AlaRS editing domain active site. To guide the design of mutagenesis experiments, we used the related AlaX−serine complex (*37*) as a model for interactions of the AlaRS editing domain with its amino acid substrate. While the isolated editing domain of *E. coli* AlaRS and the stand-alone AlaX proteins both exhibit robust deacylation function in vitro (*18*, *37*), for neither has editing function been fully characterized with respect to steady-state kinetics. Employing structure-based alignments of full-length AlaRS and AlaX proteins, residues predicted to be important for distinguishing between serine and alanine were identified. Substitutions were introduced at these residues, and then the resulting mutant proteins were characterized in deacylation assays employing both misacylated Ser-tRNA^{Ala} and cognate Ala-tRNA^{Ala} substrates. The results of these studies, coupled with a reexamination of AlaRS structural alignments, suggest a new model for how AlaRS achieves discrimination between serine and alanine.

EXPERIMENTAL PROCEDURES

Protein Mutagenesis, Purification, and Characterization. The plasmid encoding for histidine-tagged AlaRS was the kind gift of Karin-Musier Forsyth. Mutagenesis of AlaRS was carried out using the QuickChange system (Stratagene), and oligodeoxynucleotides were purchased from Operon. Mutagenesis results were confirmed by sequencing at the Vermont Cancer Center DNA Analysis Facility (University of Vermont). Histidine-tagged AlaRS was expressed and purified as described (*30*). Active site concentrations were determined by the active site titration assay (Supporting Information Figure S1) (*40*).

tRNA Transcription. The basic procedures for transcription and purification have been described previously (*40*, *41*). A plasmid carrying the tRNA^{Ala} gene under the T7 RNA polymerase (RNAP) promoter was the kind gift of Karin-Musier Forsyth. Plasmids were purified from *E. coli* with the Giga kit system (Qiagen) and restricted with *Bst*N1 (New England Biolabs). Transcription reactions were composed of 40 mM Tris-HCl (pH 7.8 at 37 °C), 22 mM $MgCl_2$, 0.1% Triton X-100, 1 mM spermidine, 10 mM DTT, 1.5 mM each ATP, CTP, GTP, and UTP, 50 nM DNA template, and 50 nM T7 RNAP (*40*). RNA transcripts were precipitated with ethanol, resuspended in TE/formamide, and purified on 12% acrylamide (1:19 acrylamide:bisacrylamide), 6 M urea, Tris−borate−EDTA gels. RNAs were eluted from gel slices with an Elutrap apparatus (Whatman/Schleicher & Schuell). The concentration of functional tRNA was determined according to eq 1.

tRNA Labeling and Aminoacylation Assays. tRNAs were labeled at A76 with ^{32}P as described (*42*). Alanyl-tRNA^{Ala} was prepared in reactions composed of 50 mM Hepes (pH 7.5), 10 mM $MgCl_2$, 100 mM KCl, 5 mM β-mercaptoethanol, 2 mM ATP, 20−30 μM tRNA^{Ala}, 0.5 pM ^{32}P-labeled tRNA^{Ala}, 2 mM alanine, and 100 nM AlaRS. Reactions were incubated at 37 °C for 15 min and extracted with phenol and then with chloroform. The aminoacyl-tRNA was purified by gel filtration chromatography (Illustra NAP-5; GE Healthcare) and then stored at −80 °C. To determine the concentration of tRNA in the fractions, aliquots from the aminoacylation reaction (before extraction with phenol) and each column fraction were spotted on TLC plates and quantitated using a Bio-Rad model FX phosphorimager. To determine the concentration of aminoacylated tRNA, aliquots were treated with S1 nuclease in 10 μL reactions composed of 40 mM sodium acetate (pH 5.0), 300 mM NaCl, 2 mM $ZnSO_4$, and 1 unit/mL S1 nuclease (Fermentas). Reactions were incubated at 22 °C for 1 h, and then 1 μL aliquots were analyzed by thin-layer chromatography on PEI cellulose plates (Sigma or EMD). The mobile phase consisted of 0.1 M ammonium acetate/5% acetic acid. The concentration of aminoacylated tRNA was determined according to eq 1:

$$[\text{aa-tRNA}] = \frac{\text{aa-Ap}[\text{tRNA}]_{\text{total}}}{(\text{aa-Ap} + \text{Ap})} \quad (1)$$

where aa-Ap is the amount of aminoacylated A76 and Ap is the amount of nonaminoacylated A76, both quantified by phosphorimager analysis. $[tRNA]_{total}$ was measured by optical absorbance at 260 nm. Seryl-$tRNA^{Ala}$ was prepared by aminoacylation reactions as described above, except that 0.75 M serine was substituted for alanine and 300 nM AlaRS C666A was substituted for AlaRS WT.

Aminoacyl-tRNA Deacylation Assays. Deacylation assays included 50 mM HEPES (pH 7.5), 10 mM $MgCl_2$, 100 mM KCl, 5 mM 2-mercaptoethanol, aminoacylated $tRNA^{Ala}$ (prepared as described in the text), and 5 nM AlaRS. Reactions were incubated at 37 °C. Aliquots were quenched in 3−5 volumes of 3 M sodium acetate (pH 5.0) and precipitated with 3 volumes of ethanol. Pellets were washed with 75% ethanol, dissolved in 10 μL of S1 nuclease reaction mix, and analyzed by TLC as described above. The amount of aminoacylated tRNA remaining at time t was calculated by eq 2:

$$\text{aa-Ap}_{\text{pmol}} = \frac{\text{aa-Ap}_{\text{I}}(\text{aa-tRNA})_{\text{pmol}}}{(\text{aa-Ap}_{\text{I}} + \text{Ap}_{\text{I}})} \quad (2)$$

where $\text{aa-Ap}_{\text{pmol}}$ is the amount of acylated A76 (in picomoles) remaining at a given time point, Ap_{I} is the intensity in phosphorimager units of the spot corresponding to deacylated A76, (aaAp_{I} + Ap_{I}) is the sum of the intensities of the spots corresponding to aminoacylated and deacyalated A76, and $(\text{aa-tRNA})_{\text{pmol}}$ is the amount of aminoacylated tRNA at time zero in the reaction. Equation 2 takes into account our observations that aminoacyl-tRNA stored at −80 °C underwent some degree of deacylation. To determine initial reaction velocities, time course data (corresponding to the first 1−2 min of the reaction for Ser-$tRNA^{Ala}$ and the first 5−7 min for Ala-$tRNA^{Ala}$) were fit to a linear regression using Microsoft Excel version 12.2.5 or KaleidaGraph version 4.03. The initial rates in picomoles per second were divided by the concentration of enzyme in the reaction to generate final velocities, which then were plotted against substrate concentrations and fit to the Michaelis−Menten equation. For a number of the mutants, and for all reactions with Ala-$tRNA^{Ala}$, saturating velocities were not reached at the highest concentrations of the aminoacylated tRNA substrate, implying an increase in the K_M parameter to values far in excess of 15 μM. Therefore, for these cases, only the apparent second-order rate constants (k_{cat}/K_M) are reported, which were derived from the slopes of the velocity versus [tRNA] plots. Deacylation rates of Ser-$tRNA^{Ala}$ and Ala-$tRNA^{Ala}$ in the absence of enzyme were determined by fitting the progress curves to equations describing a first-order decay.

RESULTS

Modeling the E. coli AlaRS Editing Active Site. The complex of *Pyrococcus horikoshii* AlaX with serine (*37*) provides a model of the AlaRS editing domain with noncognate serine (Figure 1). We created a manual 3-D alignment of this structure with the editing domains of full-length *P. horikoshii* AlaRS (*27*) and full-length *Archaeoglobus fulgidis* (*26*) AlaRS, minimizing the rmsd of the conserved secondary structures in the domain using Pymol (*43*). This structural superposition was then used to manually edit a ClustalW sequence alignment of the above referenced sequences with those corresponding to *P. horikoshii* AlaRS, *E. coli* AlaRS, and *Homo sapiens* AlaRS. The end result was essentially equivalent to the alignment published in ref *26*. This information allowed us to predict, relative to the AlaX

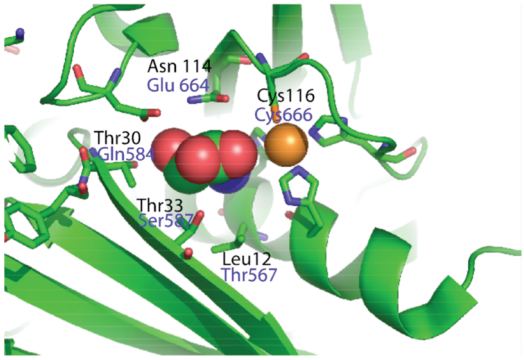

FIGURE 1: Mutagenesis of the AlaRS editing active site. The active site of *P. horikoshii* AlaX complexed with zinc (orange sphere) and serine (space-filling model) is shown. Side chains adjacent to the serine are labeled in black for *P. horikoshii* AlaX, while their inferred equivalents in *E. coli* are indicated in blue. Structural overlays of the AlaX with *P. horikoshii* AlaRS and *A. fulgidis* AlaRS, along with sequence alignment of *P. horikoshii* AlaRS, *E. coli* AlaRS, and *H. sapiens* AlaRS, were used to identify comparable *E. coli* AlaRS residues at the editing active site (also see ref *37*).

structure, residues in the *E. coli* AlaRS editing active site that may be involved in contacts to the α-carboxylate and the β-hydroxy groups of the serine substrate (Table 1). The latter would be predicted to be important in differentiating alanine from serine. In addition, we identified Ile677 in *E. coli* AlaRS as the specific residue that aligns with Ala734 in mouse AlaRS; the A734E mutation is associated with the "sticky mouse" phenotype (*39*).

The mutant substitutions were chosen to prevent the targeted residues from making the predicted contacts suggested by the *P. horikoshii* AlaX structure (Figure 1). Among those contacts, Thr30 is predicted to be a critical discriminating interaction for the β-hydroxy moiety of serine. In *E. coli* AlaRS, Gln584 is predicted to be the residue that aligns with AlaX T30, and this motivated the construction and characterization of Q584N, Q584H, and Q584A AlaRS. In AlaX, Leu12 is predicted to make a close contact with the α-carbon of serine, thereby defining part of the steric features of the substrate binding pocket for the amino acid (Figure 1). In the *E. coli* enzyme, the corresponding residue is Thr567, which also has the potential to engage in a hydrogen bond with the β-hydroxyl of serine. To test the importance of this interaction, T567 was substituted with glycine. Asn114 of *P. horikoshii* AlaX makes a steric contact with another face of the serine substrate. Because Glu664 represents the equivalent residue in *E. coli*, it was substituted with alanine. The remaining substitutions introduced into the *E. coli* enzyme were Cys666A and I677E. The former abolishes one of the residues predicted to coordinate the zinc atom in the editing site, while the latter substitutes the residue in *E. coli* AlaRS which aligns with Ala734 in mouse and human AlaRS.

Deacylation Assays. Each of the resulting mutant enzymes was then tested for deacylation function, employing $tRNA^{Ala}$ aminoacylated with either cognate amino acid substrate alanine or with the near-cognate substrate serine. The preparation of Ala-$tRNA^{Ala}$ deacylation substrates was accomplished using wild-type AlaRS, while Ser-$tRNA^{Ala}$ was produced using C666A AlaRS, which prior work had suggested is severely reduced for editing function (*36*). To maximize the amount of $tRNA^{Ala}$ produced and the sensitivity of the quantitation, all tRNAs were labeled at their 3′-terminal adenosine (A76) nucleotide with ^{32}P using the Wolfson−Uhlenbeck method (*42*, *44*). Deacylation assays were then performed under steady-state conditions using

Table 1: Equivalent Positions in the AlaRS Editing Active Site As Inferred from Multiple Sequence Alignments[a]

predicted contact to Ser-tRNA^{Ala} substrate	*P. horikoshii* AlaX	*E. coli* full-length AlaRS	*H. sapiens* full-length AlaRS	*P. horikoshii* full-length AlaRS	*A. fulgidis* full-length AlaRS
main chain					
α-amino group	His13	His568	His609	His617	His604
α-carboxyl group	Asn114	**Glu664** (**Ala**)	Glu721	Gln715	Gln701
α-carboxyl group	Cys116	**Cys666** (**Ala**)	Cys723	Cys717	Cys703
α-carboxyl group	Thr33	Ser587	Ser627	Ser636	Ala623
α-carbon	Leu12	**Thr567** (**Gly**)	Thr608	Thr616	Thr603
side chain					
contacts hydroxyl R-group	Thr30	**Gln584** (**His**, **Asn**, **Ala**)	Gln624	Gln633	Gln620
contacts hydroxyl R-group)	Asp92	Phe645	Phe686	Gln695	Gln682
"sticky mouse" linked mutation	Ile127	**Ile677** (**Glu**)	Ala734	Val728	Ile714

[a]Substitutions introduced into the residues of interest examined in this study are indicated in parentheses.

varying tRNA concentrations, with the extent of deacylation being determined by separation and quantitation of the reaction products by TLC. This experimental design permitted the K_M and k_{cat} parameters to be determined independently, except for those mutants where [tRNA] saturation could not be achieved at concentrations up to 15 μM.

The results of these assays for deacylation of Ser-tRNA^{Ala} are shown in Figure 2 and Table 2. Wild-type (WT) AlaRS exhibited well-behaved Michaelis−Menten kinetics with respect to increasing mischarged tRNA substrate concentrations, allowing apparent K_M (5.0 μM) and k_{cat} (3.3 s^{-1}) parameters to be determined (Table 2). The AlaRS mutants could be divided into two groups on the basis of their deacylation activities. Two of the mutants, T567G and E664A AlaRS, exhibited near wild-type levels of deacylation function. Both showed saturation behavior with respect to increasing tRNA^{Ala} concentrations, and their second-order rate constants were less than 2-fold changed relative to wild-type AlaRS. The individual parameters for E664A AlaRS (K_M = 6.3 μM and k_{cat} = 4.6 s^{-1}) were not more than 2-fold greater than those of wild type, while the individual k_{cat} and K_M parameters of T567G (K_M = 1.9 μM and k_{cat} = 0.8 s^{-1}) were both reduced in the range of 3−4-fold relative to wild-type AlaRS. Thus, among the two mutants, the T567G mutation had the greater effect, increasing the apparent substrate binding affinity and decreasing the rate of hydrolysis.

The mutant proteins Q584H, C666A, and I667E AlaRS were all significantly less active in deacylation function than T567G and E664A. None of them exhibited saturation behavior with respect to increasing concentrations of tRNA^{Ala}, effectively preventing the determination of individual K_M and k_{cat} parameters (Figure 2). However, the linear response of velocity to increasing tRNA^{Ala} concentrations allowed the second-order rate constant k_{cat}/K_M to be derived from the slopes of these plots. Q584H, Q584A, and I677E AlaRS returned k_{cat}/K_M values of 1.1 × 10^5, 2.9 × 10^5, and 1.0 × 10^5 M^{-1} s^{-1}, which are approximately 3−6-fold lower than the corresponding value of 6.6 × 10^5 s^{-1} M^{-1} determined for wild-type AlaRS. By contrast, Q584N AlaRS was more active, with a k_{cat}/K_M of 6.1 × 10^5 M^{-1} s^{-1}, which was close to the value recorded for wild-type AlaRS (Supporting Information Figure S2, Table 2). Similar to Q584H, C666A, and I667E AlaRS, however, the velocity versus [S] plot for this mutant did not show saturation behavior with respect to increasing tRNA. The C666A mutant also did not exhibit saturating Michaelis−Menten kinetics, and a value of 4.4 × 10^4 M^{-1} s^{-1} was determined for k_{cat}/K_M (Table 2). This represents a 15-fold decrease relative to the value for wild-type AlaRS.

Specificity of the AlaRS Editing Domain. The catalytic efficiency of deacylating Ser-tRNA^{Ala} represents one metric for assessing the functional contributions of the residues substituted in these experiments. However, this parameter alone provides no information about the deacylation of Ala-tRNA^{Ala}, which is not expected to be a substrate for wild-type AlaRS editing. To assess the editing specificity of the various mutants, deacylation experiments were also performed using Ala-tRNA^{Ala} as substrate. Relative to the activity on near-cognate seryl-tRNA^{Ala}, the hydrolysis of cognate Ala-tRNA^{Ala} was slower with the wild type and, with the exception of C666A AlaRS, all mutant AlaRS. In all cases, including wild-type AlaRS, a saturating velocity was not reached at tRNA concentrations up to and including 12 μM, indicating that the affinity of the AlaRS editing site for cognate Ala-tRNA^{Ala} is relatively poor (Figure 3). With exception of Q584N AlaRS, the second-order rate constants for the deacylation catalyzed by wild-type AlaRS and the mutants were in the range of 4.9−7.4 × 10^4 M^{-1} s^{-1} (Table 2). Notably, Q584N and C666A AlaRS both showed a high rate of deacylation of Ala-tRNA^{Ala}, relative to their activity on Ser-tRNA^{Ala}.

The availability of these parameters allowed the specificity of the editing function of the wild-type and the mutant AlaRS to be calculated directly from the ratio of $(k_{cat}/K_M)_{Ser}/(k_{cat}/K_M)_{Ala}$, which would be unity if AlaRS editing lacked specificity for mischarged tRNA. The calculated specificity values range from a high of 12.2 for wild-type AlaRS to a low of 0.6 (Table 2). Two mutants, T567G and E664A AlaRS, exhibited values (9.2 and 11.2, respectively) that were quite similar to wild type, while the ratio for I677E and Q584H AlaRS was reduced to just 1.5 and 1.9, respectively. C666A AlaRS, the least active in deacylation of Ser-tRNA^{Ala}, was the sole mutant with a ratio less than 1, representing the only instance where Ala-tRNA^{Ala} is the preferred substrate.

To permit calculation of the rate enhancement provided by the enzyme, relative to the uncatalyzed reaction, the rates of enzyme-independent solution hydrolysis of Ala-tRNA^{Ala} (Figure 4) and Ser-tRNA^{Ala} (not shown) were determined. The measured first-order rate constants of enzyme-independent deacylation for Ser-tRNA^{Ala} and Ala-tRNA^{Ala} were 1 × 10^{-4} s^{-1} and 4 × 10^{-4} s^{-1}, respectively. Relative to the uncatalyzed reaction, therefore, AlaRS at a concentration of 1 μM enhances the rate of Ser-tRNA^{Ala} hydrolysis by a factor of only 6000. This can be compared to the value of 100 calculated for the rate enhancement of AlaRS-catalyzed deacylation of Ala-tRNA^{Ala} relative to the uncatalyzed solution

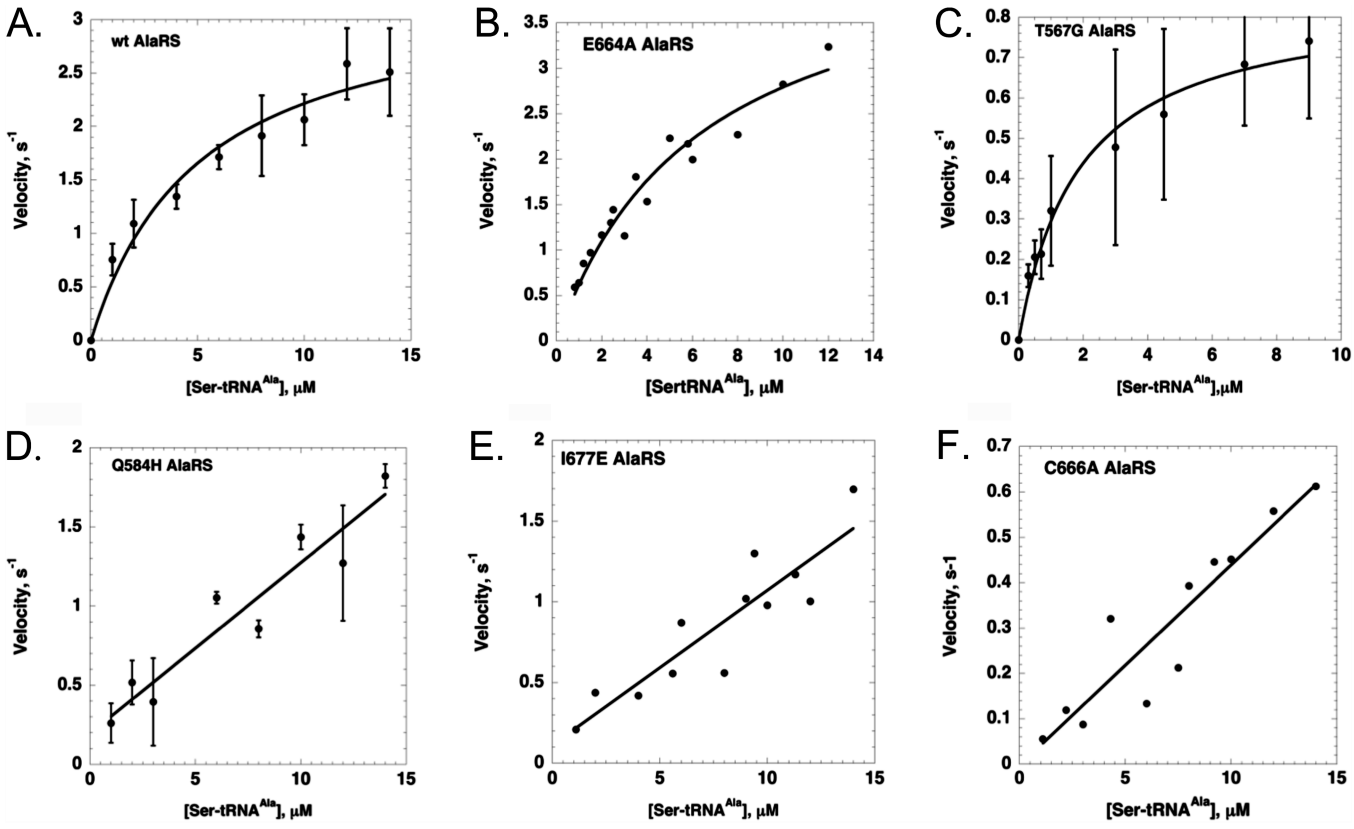

FIGURE 2: Editing of seryl-tRNA^{Ala} with AlaRS WT and editing mutants. Measurements of editing initial rates with AlaRS WT, T567G, and E664A versus [seryl-tRNA^{Ala}] were fit to the Michaelis−Menten equation, whereas data obtained with AlaRS Q584H, C666A, and I677E were fit by linear regression. The resulting k_{cat}, K_M, and/or k_{cat}/K_M parameters are reported in Table 2. The rates shown represent an average of two to four independent measurements. Error bars, when shown, represent the standard of at least three independent measurements. When no errors bars are shown, each rate represents the average of two independent experiments, with a variance of no more than 25%.

Table 2: Steady-State Kinetic Parameters for Deacylation of aa-tRNA^{Ala} at 37 °C and pH 7.5[a]

AlaRS	seryl-tRNA^{Ala}, k_{cat} (s^{-1})	seryl-tRNA^{Ala}, K_M (10^{-6} M)	seryl-tRNA^{Ala}, k_{cat}/K_M (10^5 M^{-1} s^{-1})	alanyl-tRNA^{Ala}, k_{cat}/K_M (10^5 M^{-1} s^{-1})	$(k_{cat}/K_M)_{Ser}/(k_{cat}/K_M)_{Ala}$
WT	3.3 ± 0.3	5.0 ± 1.4	6.6	0.54	12.2
E664A	4.6 ± 0.4	6.3 ± 1.1	7.3	0.65	11.2
T567G	0.8 ± 0.1	1.9 ± 0.3	4.5	0.49	9.2
Q584N	ND[b]	ND	6.1	5.0	1.2
Q584A	ND	ND	2.9	1.4	2.1
Q584H	ND	ND	1.1	0.57	1.9
I677E	ND	ND	1.0	0.67	1.5
C666A	ND	ND	0.44	0.74	0.6

[a]For the WT, T567, and E664 enzymes with the noncognate seryl-tRNA^{Ala} editing substrate, the k_{cat} and K_M values were obtained from the Michaelis−Menten plot. For the I677E, C666A, Q584H, Q584N, and Q584A AlaRS mutants, the k_{cat}/K_M constants were derived from the slopes of the V versus [tRNA] plots. For all experiments employing the cognate alanyl-tRNA^{Ala} as substrate, the k_{cat}/K_M constants were derived from the slopes of the V versus [tRNA] plots. [b]ND, not determined, owing to failure to reach saturation with respect to tRNA binding.

value. The modest nature of these values has interesting biological and evolutionary implications.

DISCUSSION

Steady-State Parameters of Ser-tRNA^{Ala} Editing by AlaRS. By its use of ^{32}P-labeled tRNA substrates instead of the more common ^{3}H- or ^{14}C-labeled amino acids, the Wolfson−Uhlenbeck assay allows higher concentrations of misacylated tRNA to be prepared and allows deacylation kinetics to be quantitated accurately. Employing this assay, the steady-state parameters of AlaRS deacylation were readily determined (Table 2). For Ser-tRNA^{Ala}, the observed values (k_{cat} = 3.3 s^{-1} and K_M = 5.0 μM) are close to the k_{cat} of 1.4 s^{-1} and 2.8 μM reported for the K_M for aminoacylation of tRNA^{Ala} by AlaRS (*45*), and the K_D of 3 μM for tRNA^{Ala} from the full-length AlaRS recently reported (*30*). The similarity in values for the K_M for tRNA^{Ala} in the aminoacylation and deacylation reactions may not be overly surprising, given that the tRNA structure is likely to provide the majority of ground state binding free energy in both reactions.

It should be noted, however, that the parameters reported here refer only to the deacylation reaction, which may not be equivalent to a *cis*-editing reaction in which the aminoacyl-CCA end of misacylated tRNA formed *in situ* is translocated to, and then

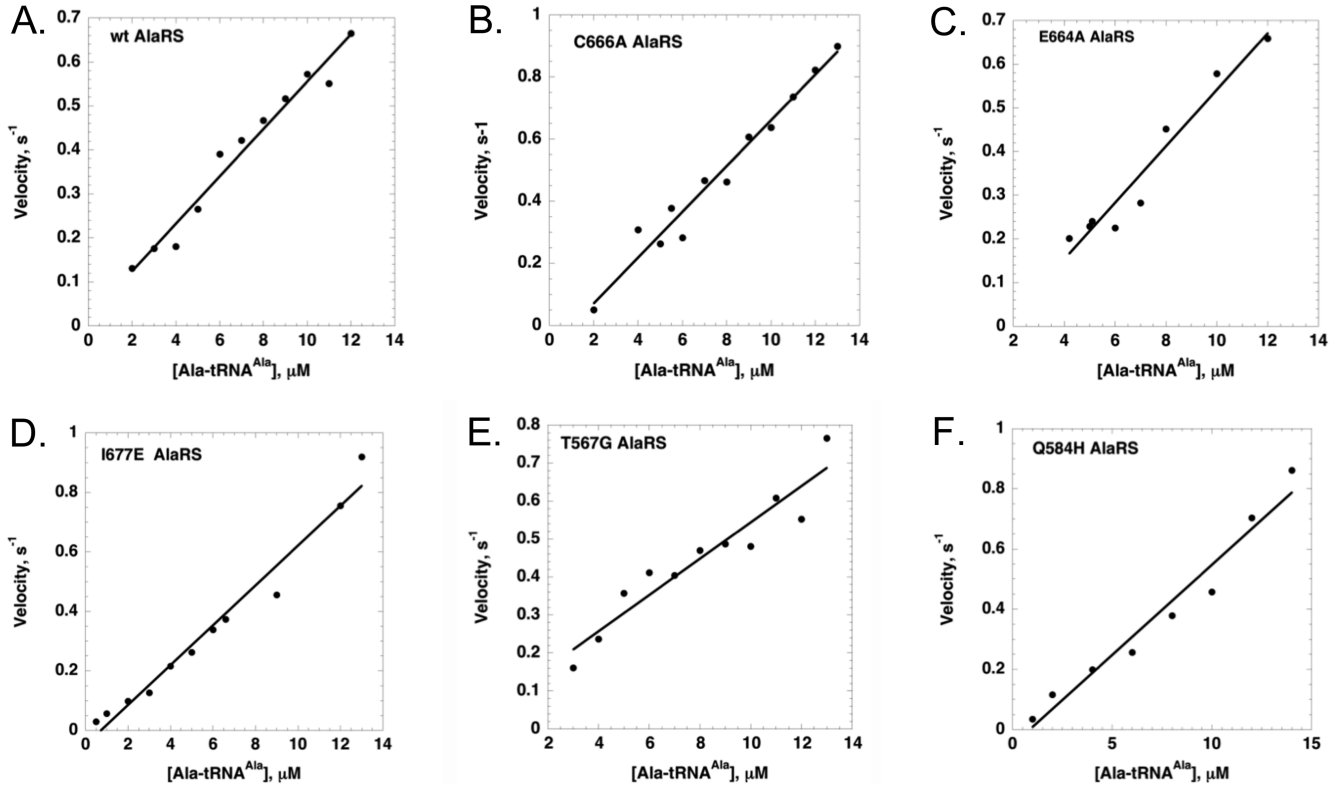

FIGURE 3: Deacylation of alanyl-tRNA^{Ala} with the AlaRS WT and editing mutants. The data for each protein were plotted as in Figure 2 and fit by linear regression as described in Experimental Procedures.

deacylated in, a specialized editing site. For all ARSs, and AlaRS in particular, the degree to which editing in *cis* (i.e., direct translocation of the misacylated CCA end between the synthetic and editing site) predominates over editing in *trans* (i.e., through the sequence of dissociation, rebinding, and catalytic process recently referred to as "resampling") has not been clearly resolved (*46*). Nevertheless, the near equivalence of the parameters measured here to the previously measured k_{cat} for aminoacylation indicates that, for AlaRS, "resampling" could plausibly occur in a kinetically competent manner. The determination of similar parameters for the isolated AlaX domains will be valuable in assessing whether or not they can perform a similar function (*17*).

The data reported here contribute new insights into the issue of catalytic efficiency and substrate specificity of the editing domain of AlaRS. Based on the comparison of enzyme-catalyzed to solution-catalyzed deacylation of Ser-tRNA^{Ala}, the rate of enhancement of editing by AlaRS is a relatively modest 6×10^3, some six logs decreased relative to the rate enhancement of the aminoacylation reaction (*47*). The relatively inefficient nature of the AlaRS editing reaction may account for the widespread distribution of AlaX proteins, which are AlaRS-related stand-alone editing domains found in all three kingdoms of life (*17*). A further notable observation is the relatively modest ratio (i.e., 12.2) of the deacylation efficiency of Ser-tRNA^{Ala} relative to that of the cognate reaction product (Table 2). Comparable values are only available for a few systems (e.g., class I LeuRS), but the trend is also toward modest specificity (*48*, *49*). While this phenomenon deserves further study, it may be that there are enough mitigating factors *in vivo* that the evolutionary selection pressure for increased discrimination power at the editing site is minimal. Specifically, the high K_M of Ala-tRNA^{Ala} in the deacylation reaction, relative to its affinity for elongation factor (*50*), may discourage the occurrence of "resampling" of the cognate aminoacyl-tRNA product (*46*).

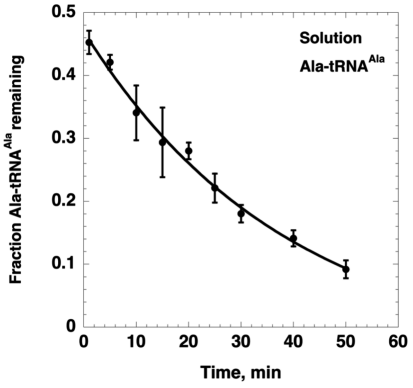

FIGURE 4: Uncatalyzed deacylation of alanyl-tRNA^{Ala}. Fraction of alanyl-tRNA^{Ala} remaining (circles) is plotted as a function of time, and the data are fit to the first-order equation (shown as a line).

Analysis of the AlaRS Editing Site. The editing sites of ThrRS and AlaRS are both characterized by conserved HXXXH and CXXXH motifs, and the introduction of mutations into these motifs decreases editing function in both systems (*36*, *51*, *52*). While there is crystallographic evidence that these motifs collaborate to constitute a zinc-binding motif in AlaRS, evidence for bound zinc is decidedly equivocal in ThrRS (*52*). In the mechanism proposed for the ThrRS-catalyzed deacylation, His73 functions as general base, while other residues in the ThrRS editing site, including Lys156 and Asp180, contribute to catalytic function through direct contacts to the A76 or seryl moieties (*52*, *53*). For AlaRS, the soaking of serine and $ZnCl_2$ into crystals of the isolated AlaX protein has provided a model for serine binding to the editing domain, although an explicit editing mechanism was

not proposed (*37*). In addition to density for the zinc atom, a bound water molecule is observed, although not at either of the positions reported for the catalytic water molecules in the ThrRS editing domain (*37*, *52*).

In the work reported here, the contacts predicted in the *P. horikoshii* AlaX complex were used to guide the mutagenesis targets in the editing site of *E. coli* AlaRS, with the expectation that the properties of the resulting mutants would validate the AlaX model. Glu664 was predicted to occupy the same position in the AlaRS editing site that Asn114 occupies in the AlaX structure, nesting directly adjacent to the serine substrate and making hydrogen bonds to the α-carboxylate and the β-hydroxyl. In view of the minimal effect on catalytic function associated with the E664A substitution (Table 2), this contact in *E. coli* AlaRS is either absent or makes no contribution to the ground or transition states. In contrast, the Thr567G substitution led to a modest decrease in k_{cat} and K_M (Table 2). As the equivalent residue in AlaX (Leu12) is predicted to make a van der Waals contact to the other face of serine, the glycine substitution may increase the included volume of the editing site, increasing the potential for nonproductive binding and thereby lowering both K_M and k_{cat} (*54*).

In the AlaX structure, the most important residue for providing specificity for Ser-tRNA^{Ala} is Thr 30, which is equivalent to Gln584 in *E. coli* AlaRS. Here, we tested three different substitutions at this position, Q584H, Q584N, and Q584A. Of the three mutants, Q584N AlaRS was the most active, with a deacylation activity on Ser-tRNA^{Ala} that was essentially equivalent to that of the wild-type enzyme (Table 2). Notably, this mutant also displayed an elevated activity on the cognate product Ala-tRNA^{Ala}, which is consistent with the prior observation by Sokabe et al., who reported that the T30V AlaX mutation increased the hydrolysis of Ala-tRNA^{Ala} without significantly affecting the hydrolysis of Ser-tRNA^{Ala} (*37*). By comparison, the other two mutants, Q584H and Q584A AlaRS, were less active than Q584N AlaRS and exhibited slightly higher specificity ratios. The failure to observe saturating velocities with all three mutants argues that Q584 is likely to be important in determining the affinity for tRNA substrate, either directly or indirectly. A direct role in catalysis is also possible. Both our results and those of Sokabe et al. differ from previous work that concluded that the Q584H mutation alone does not have significant effects on editing (*36*). It is possible that the detailed kinetic treatments of the mutants in our study may have uncovered effects missed in the previous work. While our results thus provide support for the importance of Q584 in the editing reaction, any detailed conclusions should include the caveat that our study focused on the full-length AlaRS, while the work of Sokabe et al. addressed AlaX, whose active site might be distinct from that of AlaRS.

A Conserved Cysteine in the AlaRS Editing Site Is Critical for Function. Among all substitutions tested, C666A conferred the most severe decrease in the deacylation rate for Ser-tRNA^{Ala} but did not decrease the rate of deacylation of the cognate product Ala-tRNA^{Ala} (Table 2). Further, the rate of deacylation catalyzed by C666A AlaRS showed no saturation at concentrations up to14 μM in Ser-tRNA^{Ala}, indicating that one consequence of the mutation is reduced ground state affinity for tRNA. In view of previous work showing that C666S displays an increased propensity to release bound zinc in response to chelating agents (*55*), we hypothesize that the zinc atom may participate in interactions that stabilize aminoacyl-tRNA binding. Were loss of the zinc atom to merely destabilize local protein structure, a commensurate decrease in the deacylation of Ala-tRNA^{Ala} might be expected, in contrast to our results. In the crystal structures of *P. horikoshii* AlaX, *A. fulgidus* AlaRS, and *P. horikoshii* AlaRS, the zinc ion is coordinated to three histidine side chains and a conserved cysteine that is equivalent to C666 in *E. coli* AlaRS (*26*, *27*). In the *P. horikoshii* AlaX structure, the zinc is closest to the α-carboxylate and nearly 7.25 Å from the seryl β-hydroxyl group. Based on the AlaX model, the zinc would be predicted to have little or no role in providing specificity for Ser-tRNA^{Ala} over Ala-tRNA^{Ala}. The switch in substrate specificity observed here for C666A (Table 2) is at odds with this prediction.

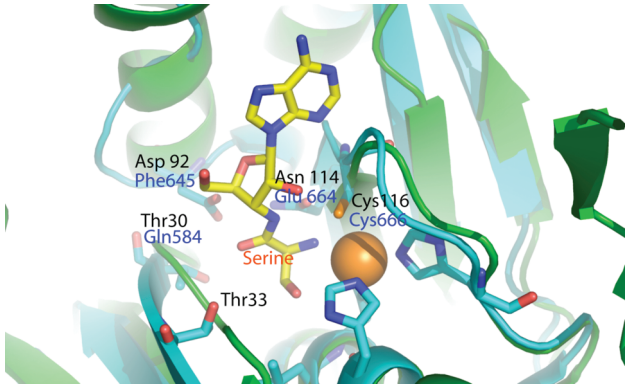

FIGURE 5: Model of seryl-adenosine in the editing active site. A structural overlay of the *P. horikoshii* AlaX (blue backbone) and *E. coli* ThrRS (green backbone) editing active sites is used to show the posttransfer editing substrate analogue serine 3-aminoadenosine in the active site of AlaX. The zinc atom, oriented toward the β-hydroxyl of serine, is shown as an orange sphere. The AlaX side chain identifiers are indicated in black type, while the corresponding *E. coli* AlaRS residues are indicated in blue.

The AlaX editing domain (1WNU) and the editing domain of *E. coli* ThrRS in complex with the posttransfer editing substrate serine 3-aminoadenosine (1TKY) (*35*) can be superposed with a rmsd of 2.8 Å over 149 residues. When the secondary structures of the two editing sites are overlaid, the seryl moiety in the ThrRS editing domain is reversed relative to its orientation in 1WNU (Figure 5), creating a different set of predicted interactions. In this alternative orientation, Cys666, which serves as a coordinating ligand for the zinc atom, recognizes both the α-amino group and the 2′-OH of the ribose ring. The seryl moiety's α-carbonyl group is predicted to contact Gln584 and Ser587. In addition, the revised model predicts that the zinc atom and Thr567 recognize the seryl β-hydroxyl group.

Located in this fashion, the zinc ion could contribute to catalytic function by either (i) providing specificity for the β-hydroxyl or (ii) polarizing the α-amino group to provide catalytic assistance. The use of the zinc to provide amino acid discrimination provides an excellent chemical solution to the problem of achieving specificity for serine, which is larger and chemically distinct from alanine. (Our studies do not address the question of how glycine is specifically recognized.) Notably, specificity for threonine over valine in the ThrRS aminoacylation site is also dictated by a coordinated zinc atom (*35*), and a coordinated zinc atom contributes to the amino acid specificity of the atypical SerRS from *Methanosarcina barkeri* (*56*).

This alternative model for the orientation of the misacylated substrate in the AlaRS editing site is also more congruent with the results of the mutagenesis and functional analysis reported here. For example, Cys666 is now seen to participate in three distinct

interactions: two are with the substrate (i.e., the 2′-OH of A76 and the α-amino group of serine), and a third is to the zinc. In view of prior data indicating that C666S may more easily release zinc, the switch in specificity seen with C666S may reflect the loss of zinc in a reasonable fraction of ARS molecules and, with it, the ability to discriminate the aminoacyl moiety at the editing site. This rationalizes the observation that C666A is the only mutant in which amino acid specificity was inverted. An important caveat is that AlaRS and AlaX may interact with Ser-tRNA^{Ala} and other potential deacylation substrates in different fashions, accounting for the discrepancy between the contacts predicted by the AlaX superposition and our functional data. Additional quantitative studies on AlaX editing will be useful in testing this model.

The Sticky Mouse Mutation. Ile677, the *E. coli* residue that corresponds to the "sticky mouse" mutation, aligns with Ile127 in *P. horikoshii* AlaX (Figure 1). The I127 δ carbon is some 13.2 Å distant from the serine β-oxygen, which is too far to exert a direct effect on either substrate binding or chemical catalysis of editing. The change in side chain polarity associated with the I677E mutation may result in an altered spatial arrangement of neighboring residues and perhaps the overall structure of the editing domain of the enzyme. Our experiments and the structural information are consistent with the interpretation that I677 has a structural role in AlaRS editing, perhaps in stabilizing a conformation (or conformations) of AlaRS that can bind seryl-tRNA^{Ala} with appropriate affinity and specificity. We therefore confirm the previous conclusion that the "sticky mouse" mutation affects editing function (*39*), observing that, in the context of the *E. coli* AlaRS structure, the effect appears to be enhanced. The modest rate enhancement of AlaRS-catalyzed deacylation, along with the significant structural consequences of substituting serine for alanine, may confer more deleterious physiological consequences for mutations on this domain than similar domains in other ARSs.

ACKNOWLEDGMENT

We thank Dr. Karin Musier-Forsyth for the gift of clones for expression and purification of *E. coli* alanyl-tRNA synthetase and tRNA^{Ala}.

SUPPORTING INFORMATION AVAILABLE

Calculation of activity of AlaRS by active site titration and velocity versus [S] plots for Q584N AlaRS and Q584A AlaRS. This material is available free of charge via the Internet at http://pubs.acs.org.

REFERENCES

1. Ibba, M., Francklyn, C., and Cusack, S., Eds. (2005) The Aminoacyl-tRNA Synthetases, Landes Bioscience, Georgetown, TX.
2. Zaher, H. S., and Green, R. (2009) Fidelity at the molecular level: lessons from protein synthesis. *Cell 136*, 746–762.
3. Ledoux, S., Olejniczak, M., and Uhlenbeck, O. C. (2009) A sequence element that tunes *Escherichia coli* tRNA(Ala)(GGC) to ensure accurate decoding. *Nat. Struc. Mol. Biol. 16*, 359–364.
4. Murakami, H., Ohta, A., and Suga, H. (2009) Bases in the anticodon loop of tRNA(Ala)(GGC) prevent misreading. *Nat. Struct. Mol. Biol. 16*, 353–358.
5. Jakubowski, H., and Goldman, E. (1992) Editing of errors in selection of amino acids for protein synthesis. *Microbiol. Rev. 56*, 412–429.
6. Fersht, A. (1979) Editing Mechanisms in the Aminoacylation of tRNA, in Transfer RNA: Structure, Properties, and Recognition (Schimmel, P., Söll, D., and Abelson, J. N., Eds.) pp 247−254, Cold Spring Harbor Laboratory, Cold Spring Harbor, NY.
7. Guth, E. C., and Francklyn, C. S. (2007) Kinetic discrimination of tRNA identity by the conserved motif 2 loop of a class II aminoacyl-tRNA synthetase. *Mol. Cell 25*, 531–542.
8. Pauling, L. (1958) The probability of errors in the process of synthesis of protein molecules, in Festschrift fur Prof. Dr. Arthur Stoll (Birkhauser, A., Ed.) pp 597−602, Birkhauser Verlag, Basel, Switzerland.
9. Loftfield, R. B., and Vanderjagt, M. A. (1972) The frequency of errors in protein biosynthesis. *Biochem. J. 128*, 1353–1356.
10. Mascarenhas, A., Martinis, S., An, S., Rosen, A. E., and Musier-Forsyth, K. (2008) Fidelity Mechanisms in Aminoacyl-tRNA Synthetases, in Protein Engineering (RajBhandary, U. L., and Koehrer, C., Eds.) Springer-Verlag, New York, NY.
11. Ling, J., Reynolds, N., and Ibba, M. (2009) Aminoacyl-tRNA synthesis and translational quality control. *Annu. Rev. Microbiol. 63*, 612–678.
12. Francklyn, C. S. (2008) DNA polymerases and aminoacyl-tRNA synthetases: shared mechanisms for ensuring the fidelity of gene expression. *Biochemistry 47*, 11695–11703.
13. Baldwin, A. N., and Berg, P. (1966) Transfer ribonucleic acid-induced hydrolysis of valyladenylate bound to isoleucyl ribonucleic acid synthetase. *J. Biol. Chem. 241*, 839–845.
14. Fersht, A. R. (1977) Editing mechanisms in protein synthesis. Rejection of valine by the isoleucyl-tRNA synthetase. *Biochemistry 16*, 1025–1030.
15. Eldred, E. W., and Schimmel, P. R. (1972) Rapid deacylation by isoleucyl transfer ribonucleic acid synthetase of isoleucine-specific transfer ribonucleic acid aminoacylated with valine. *J. Biol. Chem. 247*, 2961–2964.
16. Silvian, L. F., Wang, J., and Steitz, T. A. (1999) Insights into editing from an Ile-tRNA synthetase structure with tRNA^{Ile} and mupiricin. *Science 285*, 1074–1077.
17. Schimmel, P., and Ribas De Pouplana, L. (2000) Footprints of aminoacyl-tRNA synthetases are everywhere. *Trends Biochem. Sci. 25*, 207–209.
18. Ahel, I., Korencic, D., Ibba, M., and Soll, D. (2003) Trans-editing of mischarged tRNAs. *Proc. Natl. Acad. Sci. U.S.A. 100*, 15422–15427.
19. Korencic, D., Ahel, I., Schelert, J., Sacher, M., Ruan, B., Stathopoulos, C., Blum, P., Ibba, M., and Soll, D. (2004) A freestanding proofreading domain is required for protein synthesis quality control in Archaea. *Proc. Natl. Acad. Sci. U.S.A. 101*, 10260–10265.
20. Ling, J., So, B. R., Yadavalli, S. S., Roy, H., Shoji, S., Fredrick, K., Musier-Forsyth, K., and Ibba, M. (2009) Resampling and editing of mischarged tRNA prior to translation elongation. *Mol. Cell 33*, 654–660.
21. Fersht, A. R. (1985) Specificty and editing mechanisms, in Enzyme Structure and Mechanism, pp 347−368, Freeman, San Francisco.
22. Tsui, W.-C., and Fersht, A. R. (1981) Probing the principles of amino acid selection using the alanyl-tRNA synthetase from *Escherichia coli*. *Nucleic Acids Res. 9*, 4627–4637.
23. Putney, S. D., Royal, N. J., DeVegvar, H. N., Herlihy, W. C., Biemann, K., and Schimmel, P. (1981) Primary structure of a large aminoacyl-tRNA synthetase. *Science 213*, 1497–1501.
24. Putney, S. D., Sauer, R. T., and Schimmel, P. R. (1981) Purification and properties of alanine tRNA synthetase from *Escherichia coli*. A tetramer of identical subunits. *J. Biol. Chem. 256*, 198–204.
25. Jasin, M., Regan, L., and Schimmel, P. (1983) Modular arrangement of functional domains along the sequence of an aminoacyl-tRNA synthetase. *Nature 306*, 441–447.
26. Naganuma, M., Sekine, S., Fukunaga, R., and Yokoyama, S. (2009) Unique protein architecture of alanyl-tRNA synthetase for aminoacylation, editing, and dimerization. *Proc. Natl. Acad. Sci. U.S.A. 106*, 8489–8491.
27. Sokabe, M., Ose, T., Nakamura, A., Tokunaga, K., Nureki, O., Yao, M., and Tanaka, I. (2009) The structure of alanyl-tRNA synthetase with editing domain. *Proc. Natl. Acad. Sci. U.S.A. 106*, 11028–11033.
28. Lu, Y., and Hill, K. A. (1994) The invariant arginine in motif 2 of *Escherichia coli* alanyl-tRNA synthetase is important for catalysis but not for substrate binding. *J. Biol. Chem. 269*, 12137–12141.
29. Regan, L., Bowie, J., and Schimmel, P. (1987) Polypeptide sequences essential for RNA recognition by an enzyme. *Science 235*, 1651–1653.
30. Guo, M., Chong, Y. E., Beebe, K., Shapiro, R., Yang, X. L., and Schimmel, P. (2009) The C-Ala domain brings together editing and aminoacylation functions on one tRNA. *Science 325*, 744–747.
31. Park, S. J., and Schimmel, P. (1988) Evidence for interaction of an aminoacyl-tRNA synthetase with a region important for the identity of its cognate transfer RNA. *J. Biol. Chem. 263*, 16527–16530.
32. Hou, Y.-M., and Schimmel, P. (1988) A simple structural feature is a major determinant of the identity of a transfer RNA. *Nature 333*, 140–145.

33. McClain, W. H., and Foss, K. (1988) Changing the identity of a tRNA by introducing a G-U wobble pair near the 3′ acceptor end. *Science 240*, 793–796.
34. Beebe, K., Mock, M., Merriman, E., and Schimmel, P. (2008) Distinct domains of tRNA synthetase recognize the same base pair. *Nature 451*, 90–93.
35. Sankaranarayanan, R., Dock-Bregeon, A.-C., Romby, P., Caillet, J., Springer, M., Rees, B., Ehresmann, C., Ehresmann, B., and Moras, D. (1999) The structure of threonyl-tRNA synthetase-tRNA^{Tyr} complex enlightens its repressor activity and reveals an essential zinc ion in the active site. *Cell 97*, 371–381.
36. Beebe, K., Ribas De Pouplana, L., and Schimmel, P. (2003) Elucidation of tRNA-dependent editing by a class II tRNA synthetase and significance for cell viability. *EMBO J. 22*, 668–675.
37. Sokabe, M., Okada, A., Yao, M., Nakashima, T., and Tanaka, I. (2005) Molecular basis of alanine discrimination in editing site. *Proc. Natl. Acad. Sci. U.S.A. 102*, 11669–11674.
38. Chong, Y. E., Yang, X. L., and Schimmel, P. (2008) Natural homolog of tRNA synthetase editing domain rescues conditional lethality caused by mistranslation. *J. Biol. Chem. 283*, 30073–30078.
39. Lee, J. W., Beebe, K., Nangle, L. A., Jang, J., Longo-Guess, C. M., Cook, S. A., Davisson, M. T., Sundberg, J. P., Schimmel, P., and Ackerman, S. L. (2006) Editing-defective tRNA synthetase causes protein misfolding and neurodegeneration. *Nature 443*, 50–55.
40. Francklyn, C. S., First, E. A., Perona, J. J., and Hou, Y. M. (2008) Methods for kinetic and thermodynamic analysis of aminoacyl-tRNA synthetases. *Methods* (*Duluth*) *44*, 100–118.
41. Yan, W., Augustine, J., and Francklyn, C. (1996) A tRNA identity switch mediated by the binding interaction between a tRNA anticodon and the accessory domain of a class II aminoacyl-tRNA synthetase. *Biochemistry 35*, 6559–6568.
42. Ledoux, S., and Uhlenbeck, O. C. (2008) [3′-^{32}P]-labeling tRNA with nucleotidyltransferase for assaying aminoacylation and peptide bond formation. *Methods* (*Duluth*) *44*, 74–80.
43. DeLano, W. L. (2008) The PyMOL Molecular Graphics System, DeLano Scientific LLC, Palo Alto, CA.
44. Wolfson, A. D., Pleiss, J. A., and Uhlenbeck, O. C. (1998) A new assay for tRNA aminoacylation kinetics. *RNA 4*, 1019–1023.
45. Hou, Y.-M., and Schimmel, P. (1989) Modeling with in vitro kinetic parameters for the elaboration of transfer RNA identity in vivo. *Biochemistry 28*, 4942–4947.
46. Ling, J., Roy, H., and Ibba, M. (2007) Mechanism of tRNA-dependent editing in translational quality control. *Proc. Natl. Acad. Sci. U.S.A. 104*, 72–77.
47. Jacobsen, J. R., Prudent, J. R., Kochersperger, L., Yonkovich, S., and Schultz, P. G. (1992) An efficient antibody-catalyzed aminoacylation reaction. *Science 256*, 365–367.
48. Mursinna, R. S., Lee, K. W., Briggs, J. M., and Martinis, S. A. (2004) Molecular dissection of a critical specificity determinant within the amino acid editing domain of leucyl-tRNA synthetase. *Biochemistry 43*, 155–165.
49. Zhai, Y., and Martinis, S. A. (2005) Two conserved threonines collaborate in the *Escherichia coli* leucyl-tRNA synthetase amino acid editing mechanism. *Biochemistry 44*, 15437–15443.
50. LaRiviere, F. J., Wolfson, A. D., and Uhlenbeck, O. C. (2001) Uniform binding of aminoacyl-tRNAs to elongation factor Tu by thermodynamic compensation. *Science 294*, 165–168.
51. Dock-Bregeon, A., Sankaranarayanan, R., Romby, P., Caillet, J., Springer, M., Rees, B., Francklyn, C. S., Ehresmann, C., and Moras, D. (2000) Transfer RNA-mediated editing in threonyl-tRNA synthetase. The class II solution to the double discrimination problem. *Cell 103*, 877–884.
52. Dock-Bregeon, A. C., Rees, B., Torres-Larios, A., Bey, G., Caillet, J., and Moras, D. (2004) Achieving error-free translation; the mechanism of proofreading of threonyl-tRNA synthetase at atomic resolution. *Mol. Cell 16*, 375–386.
53. Waas, W. F., and Schimmel, P. (2007) Evidence that tRNA synthetase-directed proton transfer stops mistranslation. *Biochemistry 46*, 12062–12070.
54. Fersht, A. R. (1999) Enzyme-Substrate Complementarity and Binding Energy in Catalysis, in Structure and Mechanism in Protein Science: A Guide to Enzyme Catalysis and Protein Folding (Fersht, A. R., Ed.) pp 349−377, W. H. Freeman, New York.
55. Wu, M. X., Filley, S. J., Xiong, J., Lee, J. J., and Hill, K. A. (1994) A cysteine in the C-terminal region of alanyl-tRNA synthetase is important for aminoacylation activity. *Biochemistry 33*, 12260–12266.
56. Bilokapic, S., Maier, T., Ahel, D., Gruic-Sovulj, I., Soll, D., Weygand-Durasevic, I., and Ban, N. (2006) Structure of the unusual seryl-tRNA synthetase reveals a distinct zinc-dependent mode of substrate recognition. *EMBO J. 25*, 2498–2509.